International Journal of Adhesion and Adhesives 93 (2019) 8–18

Contents lists available at ScienceDirect

International Journal of Adhesion and Adhesives

journal homepage: www.elsevier.com/locate/ijadhadh

Influence of elevated temperatures on epoxy adhesive used in CFRP strengthening systems for civil engineering applications

J.P. Firmo[a,*], M.G. Roquette[b], J.R. Correia[a], A.S. Azevedo[a]

[a] CERIS, Instituto Superior Técnico, Universidade de Lisboa, Av. Rovisco Pais 1, 1049-001 Lisboa, Portugal
[b] A2P Consult - Estudos e Projectos, Lda, Lisboa, Portugal

ARTICLE INFO

Keywords:
A - epoxy
B - composites
C - lap-shear
C - finite element stress analysis

ABSTRACT

This paper presents experimental investigations about the influence of elevated temperatures on the mechanical behaviour of an epoxy adhesive typically used in carbon fibre reinforced polymer (CFRP) strengthening systems and numerical investigations about the influence of changes underwent by the adhesive on the response of bonded joints between CFRP strips and concrete. The experiments included shear and tensile tests at elevated temperatures (up to 120 °C) on a commercial epoxy adhesive. In both types of tests, the mechanical response of the adhesive at different temperatures was assessed, namely in terms of stress *vs.* strain curves, stiffness, strength and failure modes. The results obtained highlighted the considerable reduction of both shear and tensile properties with increasing temperatures: at 70 °C the shear and tensile strengths are both reduced to around 15% of the corresponding ambient temperature strengths, while the tensile and shear moduli can be considered negligible. Analytical formulae were fit to the test data, describing the reduction with temperature of the adhesive's tensile and shear properties. In the numerical investigations, three-dimensional finite element models were developed to simulate previous double-lap shear tests performed on concrete blocks strengthened with CFRP strips according to either the externally bonded reinforcement (EBR) or the near surface mounted (NSM) techniques, using the epoxy adhesive characterized in the present study. Two distinct modelling strategies were adopted for the concrete-CFRP bond in order to assess the relative importance of the adhesive distortion and interfacial slippage at the concrete-adhesive-CFRP interfaces in the overall slip between concrete and CFRP: (i) to explicitly simulate the adhesive, considering the mechanical properties determined in the tests and assuming a perfect bond at all interfaces; and, alternatively, (ii) to simulate the CFRP-concrete interaction by means of global bilinear bond-slip laws for different temperatures. Comparison between numerical results and test data allowed quantifying the relative importance of the adhesive distortion and of the interfacial slippage at the bonded interfaces as a function of temperature, providing a better understanding of the contribution of these two mechanisms to the CFRP-concrete bond at elevated temperature. While the former effect is the most relevant at ambient temperature, with elevated temperature the interfacial slippage at the bonded interfaces becomes the most relevant mechanism.

1. Introduction

Over the past 25 years, carbon fibre reinforced polymer (CFRP) materials have been finding increasing applications in rehabilitation and strengthening of reinforced concrete (RC) structures. This increasing interest on CFRP materials stems from their indisputable advantages over traditional materials (in particular steel), such as high strength-to-weight ratio, corrosion resistance and ease of application [1].

In spite of the above-mentioned advantages over traditional strengthening materials/techniques, in applications where structural fire ratings are required (*e.g.* buildings), the attempts to apply these strengthening systems have been hampered due to unknowns about the reduction of their mechanical and bond properties at elevated temperatures. In fact, when the glass transition temperature (T_g) of the most susceptible material to this type of action (generally the epoxy-based adhesives, which present lower T_g than that exhibited by CFRPs [2]) is reached, its mechanical properties are severely deteriorated and, consequently, the structural effectiveness of the strengthening system is substantially affected [3].

* Corresponding author.
E-mail addresses: joao.firmo@tecnico.ulisboa.pt (J.P. Firmo), maria.roquette@a2p.pt (M.G. Roquette), joao.ramoa.correia@tecnico.ulisboa.pt (J.R. Correia), adriana.azevedo@tecnico.ulisboa.pt (A.S. Azevedo).

https://doi.org/10.1016/j.ijadhadh.2019.01.027

Available online 24 January 2019

Even though the fire performance exhibited by CFRP systems is known to be poor and the bonding adhesive has been identified as the most susceptible constituent to the mechanical degradation of the system when exposed to elevated temperatures, the (limited) research available has focused mainly on the bond degradation rather than on the characterization of the mechanical properties of the adhesives themselves; further studies are clearly needed to fill this gap in current knowledge.

This paper presents experimental and numerical investigations about the influence of elevated temperatures on CFRP systems to strengthen concrete structures. In the experimental campaign the mechanical response in tension and shear of a commercial epoxy adhesive (typically used as a bonding agent in CFRP strengthening systems for RC elements) was assessed as a function of temperature. In the numerical investigation, 3D finite element (FE) models were developed to simulate double-lap shear tests previously performed by the authors on concrete blocks strengthened with CFRP strips with two alternative techniques: externally bonded reinforcement (EBR) and near surface mounted (NSM); in both strengthening techniques, the epoxy adhesive characterized in the present study was used. Two distinct modelling strategies for the concrete-CFRP bond were adopted: (i) assuming a perfect bond between all constituent materials, but explicitly simulating the bonding adhesive, considering its mechanical properties as a function of temperature as determined in the tests; and, alternatively, (ii) simulating the CFRP-concrete interaction by means of global bilinear bond *vs.* slip laws for different temperatures that are available in the literature. The main goal was to assess the relative contribution of adhesive distortion and interfacial slippage at the bonded interfaces in the overall slip behaviour of the CFRP-concrete bonded connection.

2. Literature review

The influence of temperature on the mechanical properties of bonding adhesives used in CFRP strengthening systems for RC structures has been addressed only in a very limited number of studies. Bascom and Cottington [4] reported a tensile strength reduction of 35% at 50 °C (maximum temperature tested) on an epoxy-based adhesive with a T_g of 68 °C (test method not specified). Moussa et al. [5] reported that the strength and stiffness of a commercial epoxy adhesive (T_g = 48 °C, determined through DSC) were almost negligible at 60 °C.

Besides the aforementioned experimental studies, most prior investigations have focused on the bond behaviour between concrete and CFRP strips. In general, the existing studies concerning the influence of temperature on these bonded joints showed remarkable bond strength reductions for temperatures above the adhesives' T_g. However, there are some contradictory results regarding the bond strength variation for temperatures below T_g - in fact, some studies reported bond strength increases (when compared to those at ambient temperature) [6–9], whereas in others bond strength reductions were obtained [10–14]. For instance, Wu et al. [10] and Gamage et al. [11] reported a consistent decreasing failure load with increasing temperature. In opposition, Blontrock [6] and Klamer et al. [7] conducted double-lap shear tests and reported increasing failure loads for temperatures lower than the T_g of the adhesive. It is noteworthy that in the latter studies, in which the bond strength increased at elevated temperatures below T_g, the specimens were all conditioned at elevated temperature for long durations prior to structural testing. It is thus likely that the occurrence of post-curing of the resin improved the bond performance. Further discussion is provided in [3].

A few numerical studies were conducted on this topic, comprising the development of finite element (FE) models to simulate the influence of temperature on the bond behaviour of CFRP-concrete bonded joints. In order to accurately predict the structural response of these bonded connections, such numerical analyses generally include bond *vs.* slip relations for the CFRP-concrete interfaces at elevated temperatures. The most common approach is to simulate the bond behaviour by means of bilinear [15] or non-linear bond *vs.* slip relationships [16,17] that are representative of the overall behaviour of the joints, *i.e.*, not simulating the bonding adhesive and the CFRP-adhesive and concrete-adhesive interfaces.

Klamer [8] simulated double-lap shear tests performed at elevated temperature on concrete blocks strengthened with externally bonded (EBR) CFRP strips. Two-dimensional (2D) FE models were developed using the commercial software DIANA, in which the bond between the concrete and the adhesive was simulated with bond *vs.* slip relationships. In addition, the adhesive was also explicitly modelled (linear elastic) and its Young's modulus (obtained from compression tests) was considered as temperature-dependent. For temperatures up to the adhesive's T_g (62 °C; test method not specified), a typical bi-linear bond *vs.* slip relation for ambient temperature (simulating concrete fracture) was used. For temperatures above T_g, this relation was modified to capture the change in failure mode from cohesive to adhesive; however, this procedure did not provide good results, which may be explained by the following reasons: (i) the adhesive (elastic) properties did not consider the effect of post-curing; (ii) the non-linear response of the adhesive at elevated temperature was not considered; and (iii) a perfect bond was always considered at the adhesive-CFRP interface.

Arruda et al. [18] simulated double-lap shear tests, in which the influence of the strengthening technique, either EBR or near surface mounted (NSM), on the bond behaviour with temperature was evaluated. Three-dimensional (3D) FE models were developed, using the commercial package ABAQUS, in which the global bond behaviour of the strengthening systems was simulated by means of bilinear bond *vs.* slip laws; these were derived based on an inverse analysis, in order to maximize the agreement between experimental and numerical results in terms of (i) failure loads, (ii) load *vs.* slip responses, and (iii) strain distributions along the bonded length. Besides the good agreement between numerical and experimental results, it was also possible to accurately simulate the failure modes experimentally observed.

The brief literature review presented above shows that unlike other industries, where more information is available [19], very few experimental studies are available concerning the tensile properties at elevated temperatures of bonding adhesives typically used in CFRP strengthening systems for RC structures; and, according to the best of the authors' knowledge, none focused on their shear properties in spite of their relevance. Moreover, in what concerns the investigation efforts to describe the bond behaviour between CFRP and concrete, the numerical models developed so far to simulate the CFRP-concrete interaction at elevated temperatures are also very scarce and do not explicitly simulate the shear properties of the bonding adhesives; this approach has prevented the assessment of the relative importance to the overall bond behaviour of CFRP-adhesive-concrete joints of (i) the adhesive's distortion and (ii) the interfacial slippage at the different bonded interfaces. These shortcomings were the main motivation of the present study, which aims at providing contributions to the above-mentioned topics.

3. Description of experimental programme

3.1. Description of the epoxy adhesive used

The adhesive used in the present experimental campaign is a conventional two-component epoxy adhesive typically used to bond CFRP strips to concrete, with the commercial designation *S&P Resin 220*. The adhesive has a T_g of 47 °C, determined from dynamic mechanical analyses (DMA, dual cantilever setup, heating rate of 1 °C/min, frequency of 1 Hz, oscillation amplitude of 15 μm), based on the onset of the storage modulus curve decay (*cf.* Fig. 1a), as recommended in [20]. Thermogravimetric analysis (TGA) and differential scanning calorimetry (DSC) measurements were also performed according to ISO 11357 [21], providing the mass variation and the energy changes as a function of temperature. Tests were run from ambient temperature (approximately 25 °C) to about 800 °C, in air atmosphere, at a heating rate of 10 °C/min. An inorganic content of 70% was obtained. Based on the middle temperature of the sigmoidal mass change (*cf.* Fig. 1b), the decomposition temperature (T_d) of the epoxy adhesive was defined as being approximately 380 °C.

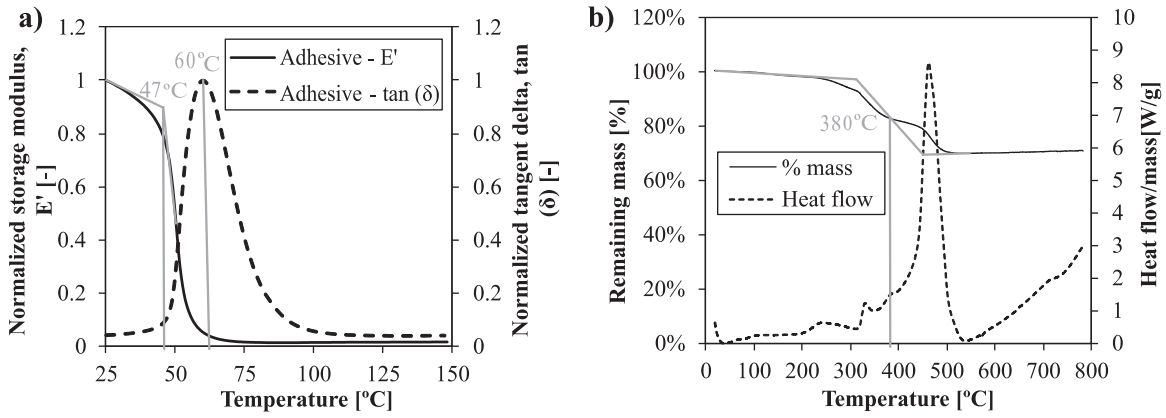

Fig. 1. a) DMA and b) DSC/TGA curves for the epoxy adhesive.

3.2. Shear tests at elevated temperatures

The shear properties of the adhesive were determined from V-notched beam, performed according to ASTM D5379 standard [22]; although this test method, also known as Iosipescu test, has been initially developed for FRP materials, it has been successfully used to assess the shear properties of bonding adhesives for civil engineering applications (*e.g.* [23,24]) and softer materials used as cores of composite sandwich panels (*e.g.* [25,26]). The coupons' geometry (*cf.* Fig. 2a) consisted of rectangular strips (75 × 20 mm, 8 mm thick) with two symmetrical centrally located V-notches. These adhesive coupons were left at 20 °C for about 7 months in order to guarantee a high-degree of ambient-temperature cure. The preparation of test specimens can be summarized in two stages: (i) the execution of a deep hole along the longitudinal direction of the specimen (17.5 mm of depth; 0.25 mm of diameter), where a thermocouple wire (type K) was introduced to measure the temperature inside the specimen; and (ii) the marking of eight reading points/targets (*cf.* Fig. 2a) used for measuring the deformations of the specimens by means of videoextensometry (as described below). As illustrated in Fig. 2b, the variation of their position was used to calculate the shear strains (γ), considering that $\gamma = \alpha + \beta$, where $\alpha = \overline{aa'}/\overline{ac}$ and $\alpha = \overline{dd'}/\overline{dc}$.

The specimens were first heated up to temperatures of 20 °C, 35 °C, 42.5 °C, 50 °C, 70 °C, 90 °C and 120 °C, in a thermal chamber (Tinius Olsen with inner dimensions 605 × 250 × 250 mm), and then load up to failure (at constant temperature) using a universal testing machine and a special test fixture (*cf.* Fig. 2c). For each temperature, at least three replicate specimens were tested. Two type K thermocouples (0.25 mm conductor diameter) were used to measure the test specimens' temperature (installed inside the drilled hole) and the air in the thermal chamber. During the heating stage the average heating rate was 14 °C/min (measured in the air inside the thermal chamber); once the predefined target temperature was attained and the coupons' temperature stabilized, the specimens were loaded up to failure under displacement control (speed of 0.5 mm/min). During the loading stage, the cross-head displacement of the test machine and the applied load were recorded, as well as the displacements of the eight points/targets (previously marked on the test specimens, *cf.* Fig. 2a) through the videoextensometry technique (*cf.* Fig. 2d), in which the following equipment was used: a high definition Sony video camera (model XCG 5005E, Fujinon – Fujifilm HF50SA-1 lens), and a computer software (LabView).

Regarding the calculation of the shear modulus, the standard test method adopted in the present study (ASTM D5379/D5379M – developed for FRP materials) recommends using the chord modulus over a 4 × 10^{-3} amplitude and for a lower bound of shear strain of 1.5 × 10^{-3} to 2.5 × 10^{-3}. However, applying this recommendation to the present test data would not allow estimating representative values for the shear modulus, especially at the higher temperatures, as the deformability of the epoxy adhesive is much higher than those figures (*cf.* Section 4.1). Therefore, in the present study, the shear modulus was estimated by the slope (obtained by linear regression) of the stress *vs.* distortion curves between 20% and 50% of the maximum shear stress. For these stress range, the response was generally linear for all tested temperatures.

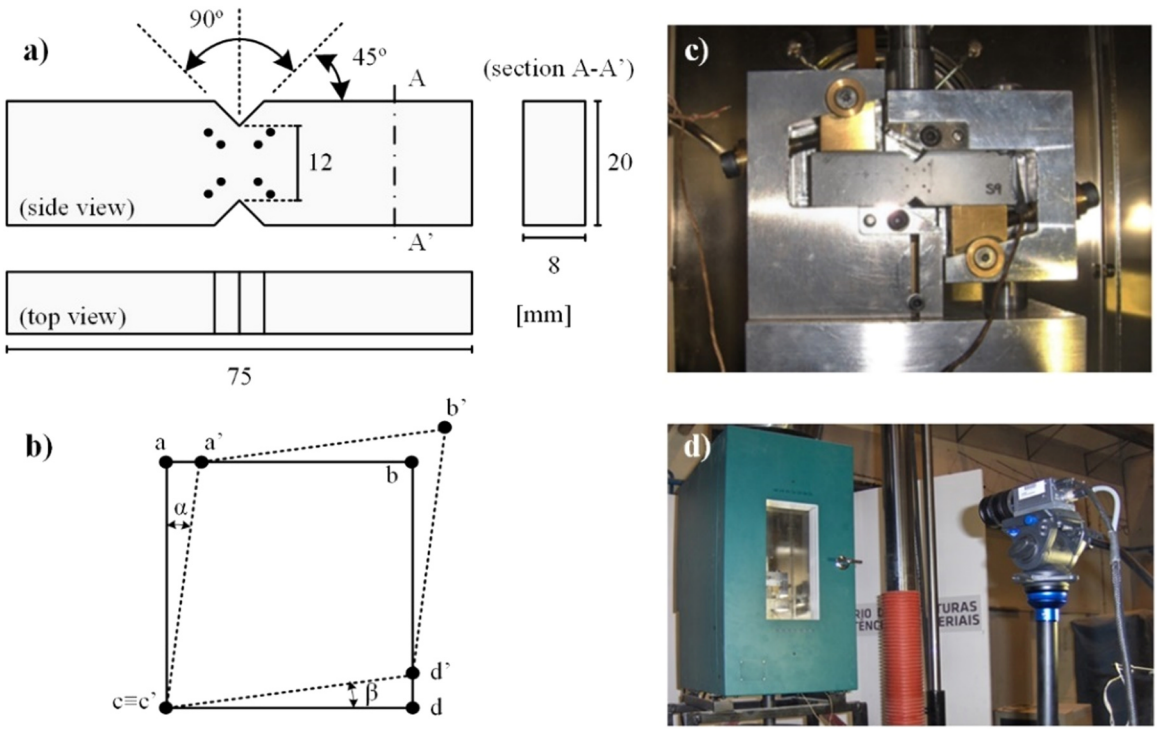

Fig. 2. Details of the shear tests: a) dimensions of the specimens and target scheme; b) shear deformation of the video extensometer targets; c) test fixture; d) video extensometer and external view of the thermal chamber.

3.3. Tensile tests at elevated temperatures

For the tensile tests, dob-bone shaped samples (*cf.* Fig. 3b) were prepared according to ISO 527-2 [27] specifications, with outer dimensions of 170 × 20 mm and 4 mm of thickness. As for the shear tests, the adhesive coupons were left at 20 °C for about 7 months in order to guarantee a high degree of ambient temperature cure. Four targets were marked on the front face of the specimens, as illustrated in Fig. 3, which were used to measure the deformations of the test specimens by means of videoextensometry.

The tensile tests, performed according to ISO 527-2 [27], were conducted by fixing both ends of the specimens between two grips, as shown in Fig. 3. For each temperature, at least three replicate specimens were tested. The procedure was similar to that adopted for the shear tests: the specimens were first heated up to temperatures of 20 °C, 35 °C, 42.5 °C, 50 °C, 70 °C, 90 °C or 120 °C, inside a thermal chamber, at an average heating rate of 16 °C/min (temperature of the air in the thermal chamber); subsequently, at constant temperature, a tensile load was applied under displacement control (speed of 0.5 mm/min) up to failure. The applied load, the cross-head displacement of the test machine and the displacements of the four points/targets marked on specimens (*cf.* Fig. 3b) were recorded. The tensile modulus was estimated using a similar criterion to that adopted for the shear modulus (*cf.* previous section), *i.e.*, by the slope (obtained by linear regression) of the axial stress *vs.* strain curves between 20% and 50% of the maximum tensile stress, a range for which the response was generally linear for all test temperatures.

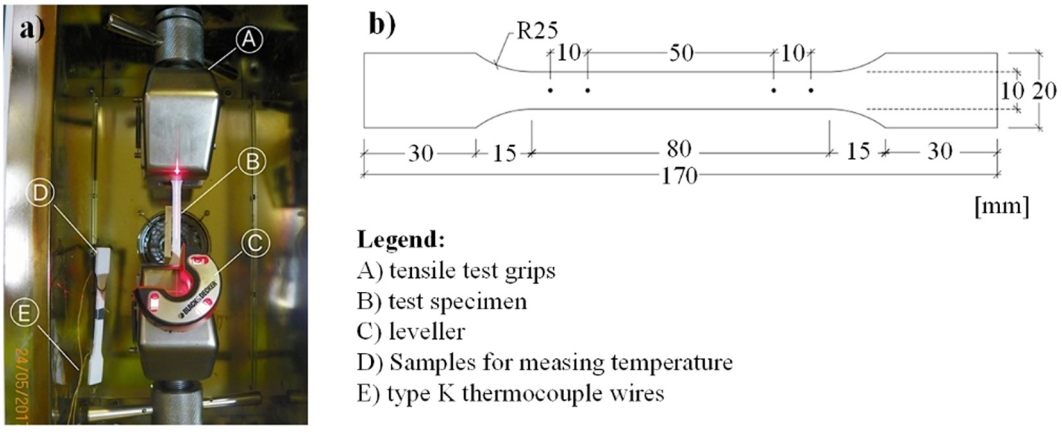

Fig. 3. Details of the tensile tests: a) general view of the tests; b) geometry of the specimens.

4. Discussion of the experimental results

4.1. Shear tests at elevated temperatures

Fig. 4 shows the shear stress *vs.* distortion curves for one representative specimen of each tested temperature. It can be observed that both the shear stiffness and strength present significant degradation with temperature (*cf.* Table 1), especially from 42.5 °C to 50 °C (*i.e.* temperature range that includes T_g - 47 °C). Furthermore, in general, an approximate linear behaviour is observed up to failure (brittle behaviour), except at 50 °C and 70 °C; for these temperatures, after the maximum shear stress is attained, there is a progressive reduction of the shear stress together with an increase in the adhesive distortion; this non-linear behaviour observed at these temperature may be related to the mechanical changes associated with the glass transition process underwent by the adhesive. Finally, it can also be seen that the maximum distortion presents a non-monotonic variation with temperature (*e.g.*, the distortion capacity increases from 42.5 °C to 50 °C, for which the viscoelasticity of the material is maximum, but decreases from 50 °C to 90 °C), unlike the variation of the maximum shear stress, which decreases monotonically with temperature.

The typical failure modes observed in the shear tests are shown in Fig. 5. In general, three types of failure were observed: (i) two inclined and parallel cracks, both beginning at the vertices of the notches (mode obtained at 20 °C, 35 °C and 42.5 °C); (ii) according to a single plane, in the central zone of the specimens (smallest cross-sectional area; mode obtained at 50 °C and 70 °C); and finally (iii) two curved cracking surfaces (mode obtained at 90 °C and 120 °C). It should be noted that these failure modes seem to be related to the behaviour of the shear stress *vs.* distortion curves: (i) test specimens whose rupture occurred with the formation of two cracks (20 °C, 35 °C, 42.5 °C, 90 °C and 120 °C) correspond to more linear curves; (ii) tests with distinct fractures (at 50 °C and 70 °C), where the rupture occurred through the central section of the specimen, correspond to non-linear curves. These different fracture patterns should be due to changes in the material behaviour (namely, the increase of viscosity and non-linearity at 50 °C and 70 °C) and the possible influence of tensile-compressive stresses in the chamfer, which should also vary with elevated temperature.

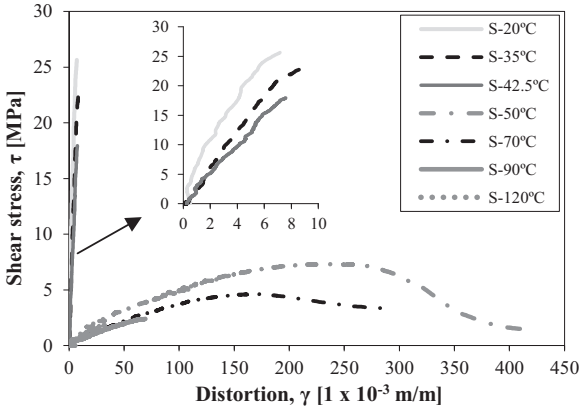

Fig. 4. Shear stress *vs.* distortion curves for representative specimens.

Table 1
Shear strength (τ_u) and modulus (G) for the different test temperatures (average ± standard deviation).

T [°C]	τ_u [MPa]	G [MPa]
20	25.1 ± 1.5	4611.1 ± 565.9
35	21.8 ± 1.8	2950.6 ± 685.8
42.5	18.4 ± 1.1	2559.9 ± 386.0
50	8.1 ± 1.3	50.5 ± 9.1
70	4.1 ± 0.5	36.2 ± 2.6
90	2.3 ± 0.3	37.8 ± 5.4
120	2.0 ± 0.3	34.5 ± 16.1

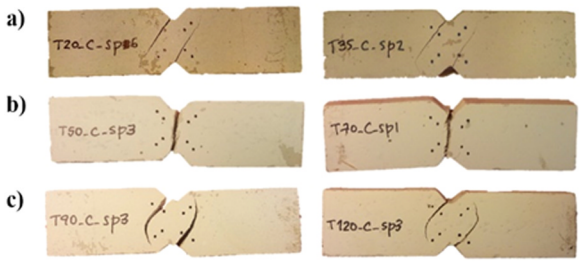

Fig. 5. Typical failure modes of specimens tested at: a) 20 °C, 35 °C and 42.5 °C; b) 50 °C and 70 °C; and c) 90 °C and 120 °C.

4.2. Tensile tests at elevated temperatures

Fig. 6 shows the axial tensile stress *vs.* strain curves, also for one representative specimen of each tested temperature. With the exception of the results obtained at 42.5 °C, which presented comparable stiffness and strength to those at 35 °C, similar conclusions can be drawn to those reported about the shear tests (*cf.* section 4.1); for instance, in addition to a remarkable stiffness reduction, the tensile strength also presents a significant degradation with temperature (*cf.* Table 2). Moreover, a change in the curves behaviour is observed as temperature increases, especially from 42.5 °C (approximately linear) to 50 °C (markedly non-linear). Finally, it can also be seen that the maximum strain presents a non-monotonic variation with temperature, unlike the variation of the maximum tensile stress, which decreases monotonically with increasing temperature.[1] Regarding the failure mode, in all test series tensile rupture at the central length of the dob-bone shaped specimens was observed.

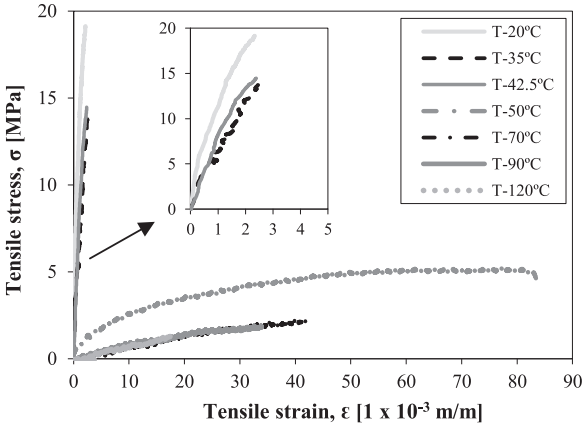

Fig. 6. Axial tensile stress *vs.* strain curves for representative specimens.

Table 2
Tensile strength (σ_u) and elastic modulus (E) for the different test temperatures (average ± standard deviation).

T [°C]	σ_u [MPa]	E [MPa]
20	16.6 ± 1.9	8205.3 ± 290.1
35	12.2 ± 1.1	6318.2 ± 594.6
42.5	12.8 ± 0.6	5970 ± 578.9
50	5.2 ± 0.1	183.2 ± 24.1
70	2.5 ± 0.2	82.9 ± 21.8
90	1.8 ± 0.2	73.0 ± 9.5
120	1.6 ± 0.3	39.5 ± 23.3

[1] The only exception were the results obtained at 42.5 °C, with both the stiffness and strength being similar to those obtained at 35 °C.

4.3. Modelling of properties degradation with temperature

Several authors have proposed mathematical expressions based on semi-empirical models to simulate the evolution of various properties of FRP materials as a function of temperature. One of the most used models is the one proposed by Gibson et al. [28], in which the variation of a generic mechanical property P with temperature T, can be described by the following equation,

$$P(T) = P_u - \frac{P_u - P_r}{2} \times (1+\tanh[k'(T - T_{g,mech})]) \quad (1)$$

where P_u is the property at ambient temperature and P_r is the property after glass transition (but before decomposition); k' and $T_{g,\ mech}$ are parameters obtained by fitting the experimental data to the equation. This section presents the calibration of Eq. (1) to the experimental data obtained in the present study for both shear and tensile properties.

Fig. 7 illustrates the normalized strength and modulus degradation curves, as well as the experimental results of the shear and tensile tests; the corresponding fitted parameters are listed in Table 3. As can be observed, a reasonable agreement between the prediction curves and the experimental results was obtained; this figure also confirms that the reduction of the stiffness properties with temperature is steeper than that exhibited by the corresponding strengths (as previously referred); in fact, both shear and tensile modulus can be considered negligible at temperatures above 50 °C. In this figure the normalized storage modulus curve, obtained from DMA tests (*cf.* Section 3.1), is also shown; although the nature of the tensile and shear tests is significantly different from that of the DMA tests, and therefore these should not be directly compared, both provide relevant information regarding the degradation of the material's stiffness as a function of temperature. For example, by comparing the curves shown in Fig. 8b), it can be seen that, according to the model of Gibson et al. [28], the most pronounced modulus reductions occur as the temperature approaches 40 °C, which is slightly lower than the adhesive's T_g (47 °C, determined from the storage modulus curve). However, it is worth mentioning that for a more detailed analysis of these comparisons one should obtain more experimental results, especially between 42.5 °C and 50 °C (range of temperatures for which the highest reductions in mechanical properties were observed).

5. Numerical modelling

5.1. Context and objectives

The structural response of CFRP-concrete bonded joints stems from (i) the contribution of both interfaces (CFRP-adhesive and adhesive-concrete), whose actual behaviour can be defined by the corresponding non-linear bond *vs.* slip laws, together with (ii) the adhesive constitutive relationship (mainly its behaviour under pure shear). However, due to the complexity of the characterization of such interfaces and materials (especially at elevated temperatures), most of the studies available in the literature simulate the bond behaviour between concrete and CFRP by simplified/global laws, representative of the overall response of the joint.

The study presented in this section comprised the numerical simulation of double-lap shear tests at 20 °C, 55 °C and 90 °C (performed by Firmo et al. [12,14]) on RC blocks strengthened with CFRP strips, applied according to either EBR or NSM techniques. The main objective of this numerical study was to assess the relative importance of the adhesive distortion and of the slippage at the CFRP-adhesive-concrete bondlines on the mechanical behaviour of the concrete-CFRP connection at elevated temperatures. To achieve this goal, two different modelling strategies for the concrete-CFRP bond behaviour were adopted: (i) to explicitly simulate the adhesive layer, using the material properties determined in this study, and neglect the bond laws at both interfaces (*i.e.* considering perfect bond at those interfaces); and (ii) to simulate the CFRP-concrete interaction by bilinear global bond *vs.* slip laws available in the literature (*i.e.* not explicitly simulating the adhesive layer). To this end, two different types of 3D finite element (FE) models were developed using ABAQUS software: (i) one model designated as "adhesive model", in which the temperature-dependent mechanical properties of the adhesive presented in Section 4 (that were independently determined) were considered, as well as those of the other materials (and perfect bond was assumed at the interfaces, to isolate the effect of adhesive distortion); and (ii) the model referred to

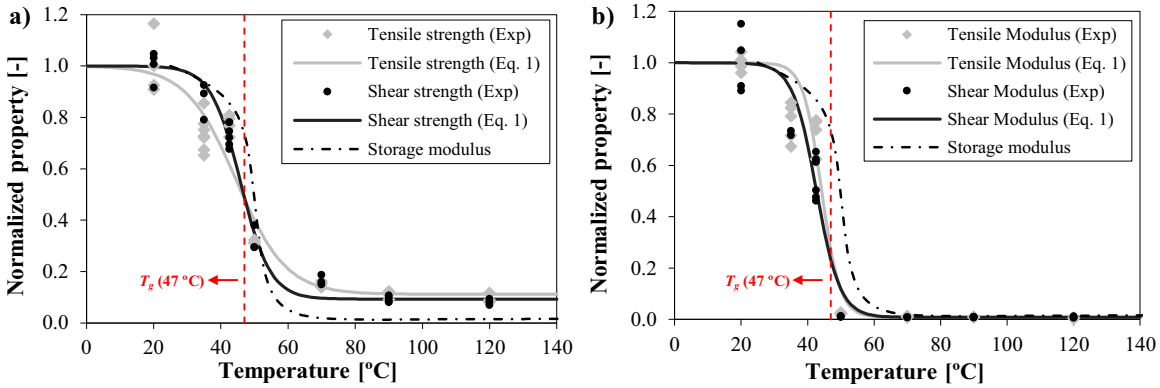

Fig. 7. Fitted curves (and experimental data) of the tensile and shear properties of the epoxy adhesive as a function of temperature in terms of a) strengths and b) stiffness.

Table 3
Parameters for the fitting of the model of Gibson et al. [28] (expression 1) to the present experimental data.

Parameter	Shear strength	Shear modulus	Tensile strength	Tensile modulus
k' [-]	0.11	0.14	0.07	0.18
$T_{g,\ mech}$ [-]	45.9	42.6	44.6	44.2

as the "interface model", in which the CFRP-concrete bond was simulated through the global bond *vs.* slip relations as a function of temperature calibrated by Arruda et al. [18]. Note that the “adhesive model” did not aim at simulating the response of the bonded joint in the brink of failure, in particular, the interface rupture, but rather at quantifying the relative influence of adhesive distortion at elevated temperature on the overall slip between concrete and the CFRP strip; given the simplifying assumptions made in this model, its outcomes are valid only for low-to-intermediate load levels, *i.e.*, before damage initiation in the materials.

In the tests performed by Firmo et al. [12,14], the specimens were first heated up to temperatures of 20 °C, 55 °C and 90 °C and then loaded up to failure (maintaining the specimens at the target temperature). Fig. 8 illustrates the geometry of the test specimens; the two concrete blocks were parallelepiped, with dimensions 120 mm × 120 mm × 350 mm and were internally reinforced with 2ϕ16 steel rebars (U-shaped, class A500NR) that were also used to apply the mechanical load. The CFRP strips were 1.4 mm thick, 20 mm wide for the EBR and 10 mm wide for the NSM, and were bonded to the concrete using the same epoxy adhesive tested in the present study. In the EBR specimens the adhesive layer was 2 mm thick, whereas in the NSM specimens, the CFRP strips were inserted into slits saw cut in the concrete cover with 15 mm of depth and 5 mm of width, as depicted in Fig. 8. The instrumentation used in the tests allowed monitoring the following parameters: (i) the load and cross-head displacement of the test machine; (ii) the slip along the bonded length of the CFRP strips (with two high-temperature LVDTs, positioned at the beginning and end of the bonded length, x = 0 and x = 250 mm, respectively; *cf.* Fig. 8); and (iii) axial strains along the bonded length of the CFRP strips.

5.2. Description of the FE models

The geometry of the FE models developed in the present study replicated that of the test specimens presented above. In order to reduce the computational costs, symmetry simplifications were adopted and only 1/8 of the test specimen volume was modelled. Fig. 9 illustrates the FE meshes of the EBR and NSM specimens, for both the interface (Fig. 9a and c) and adhesive models (Fig. 9b and d). When generating the mesh for concrete, CFRP, adhesive (1 and 5 elements throughout the thickness for the EBR and NSM adhesive models, respectively) and steel parts, 8-node hexahedral elements (C3D8R) were used. Regarding the boundary conditions, due to the symmetry simplifications, the following displacements/rotations were restricted: (i) transverse displacements (y-axis) at the loaded end of the CFRP strip; (ii) transverse displacements and rotations in the plane of symmetry xz; and (iii) transverse displacements and rotations in the plane of symmetry yz. In addition, (i) a perfect bond between the steel rebars and the concrete was assumed; and (ii) the extremity nodes of the steel rebars were fixed in all directions in order to simulate the clamps of the testing machine. A mesh sensitivity study was made.

All the constituent materials were modelled as linear elastic (without any failure criterion); the defining parameters are listed in Table 4; it is important to point out that: (i) regarding steel, the maximum stress in the reinforcement was less than half of its yield stress; (ii) regarding the concrete, for the present specimen geometry and

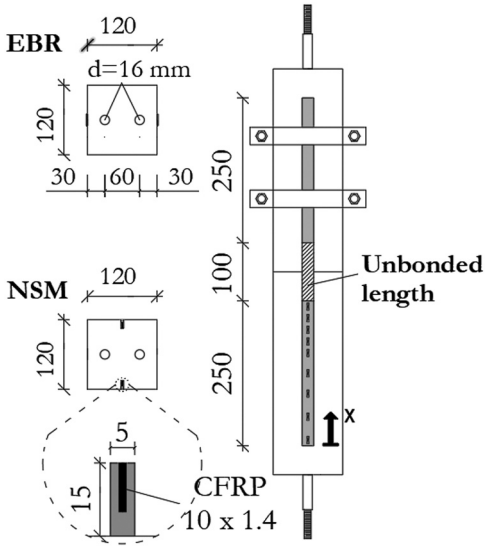

Fig. 8. Geometry of the specimens tested by Firmo et al. [12,14].

Table 4
Material properties considered in the FE models.

Material	*T* [°C]	*E* [GPa]	*G* [GPa]	*ν* [-]
Concrete	20; 55	28.7	–	0.2
	90	22.9		
Steel	20; 55; 90	200.0	–	0.3
CFRP	20; 55	152.5	–	0.3
	90	147.0	–	
Adhesive	20	8.2	4.6	0.3
	55	0.16	0.047	
	90	0.087	0.038	

materials, Arruda et al. [18] demonstrated that assuming a linear elastic model for concrete does not lead to significant losses of precision when simulating the CFRP-concrete interaction using global bond *vs.* slip laws (additionally, it considerably reduces the computational cost); and (iii) although the CFRP strips are orthotropic (comprising mainly a unidirectional reinforcement), in the present application they behave essentially in the longitudinal direction, hence, as a simplification, the CFRP was modelled as a linear elastic isotropic material.

Regarding the adhesive model, a linear elastic analysis with imposed displacement was performed. For the interface model, the concrete-CFRP bond was simulated by interface contact (in which the cohesive bilinear constitutive relationships illustrated in Fig. 10 were implemented), and included a damage initiation criterion after the maximum shear stress value is attained; such criterion corresponds to the descending branch of the bilinear relations shown in Fig. 10. In order to simulate the post-peak response, for the interface model, a static non-linear analysis was performed imposing applied displacements.

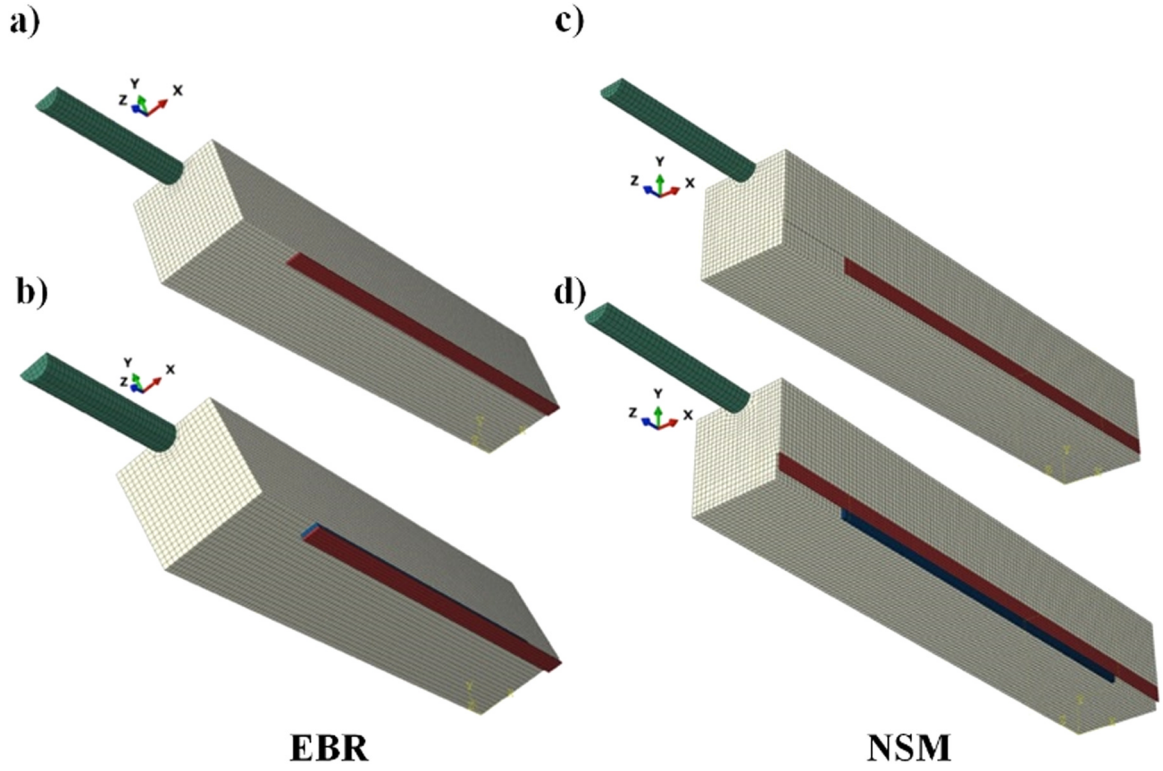

Fig. 9. a) EBR interface model; b) EBR adhesive model; c) NSM interface model; d) NSM adhesive model.

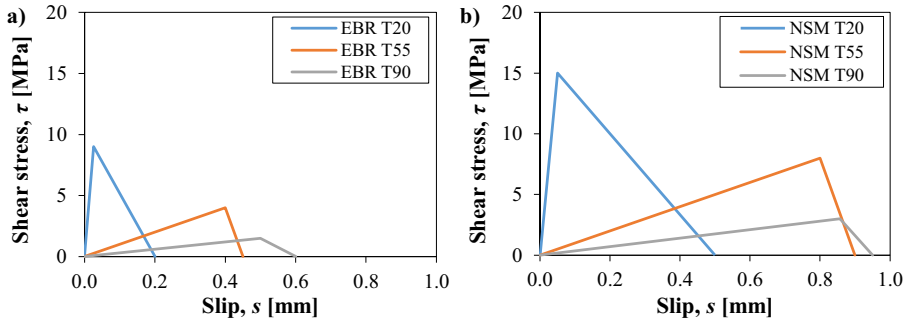

Fig. 10. Bond *vs.* slip laws for a) EBR and b) NSM interface models (from [18]).

5.3. Results and discussion

Fig. 11 depicts the numerical results of the interface and adhesive models together with the experimental results in terms of applied force *vs.* slip at the end of the bonding length (x = 250 mm, *cf.* Fig. 8) for both strengthening techniques and for all temperatures considered. Regarding the interface model at ambient temperature, for both EBR and NSM techniques, the numerical models were able to accurately reproduce the non-linear behaviour of the curves, including the stiffness reduction observed in the brink of collapse. With increasing temperatures, besides the continuous stiffness reduction obtained, the numerical curves presented a behaviour closer to linear, similar to that exhibited by the corresponding experimental curves.

Regarding the adhesive model, at ambient temperature, the initial stiffness of the numerical curves is similar to the experimental ones for both strengthening systems. This result shows that, at ambient temperature and for relatively low loads, the adhesive distortion assumes a more significant relevance for the concrete-CFRP slip value than the slippage at the concrete-adhesive and adhesive-CFRP interfaces (which were not simulated in this model). Thus, it can be concluded that, under these conditions (ambient temperature and relatively low loads), the slip at both interfaces may be considered negligible, which is logical. As temperature increases, in general, the stiffness of the curves obtained from the adhesive model become higher than the experimental ones, confirming the relevance of the slip at both interfaces and its importance to the overall structural response (a single exception occurs for the EBR system at 55 °C, for which the stiffness predicted by the adhesive model is still very similar to the experimental one).

Figs. 12 and 13 present the axial strain distributions along the CFRP bonded length obtained from the interface and adhesive models, for different fractions of the failure load and temperatures. Regarding the interface model, the figures show that there is a good agreement between experimental and numerical results. The global bond *vs.* slip relations allowed to simulate the non-linear response of the corresponding curves at ambient temperature, with null deformations at the beginning of the CFRP strip and a peak at the opposite extremity (x = 0 and x = 250 mm, respectively; *cf.* Fig. 8). For elevated temperatures, it can be seen that the axial strain distributions along the bonded length become closer to linear (*i.e.*, there is no longer a peak at the top extremity of the CFRP strip) and a reduction of the overall magnitude of the strain distributions as temperature increases. These results are mainly explained by the stiffness reduction of the adhesive and the

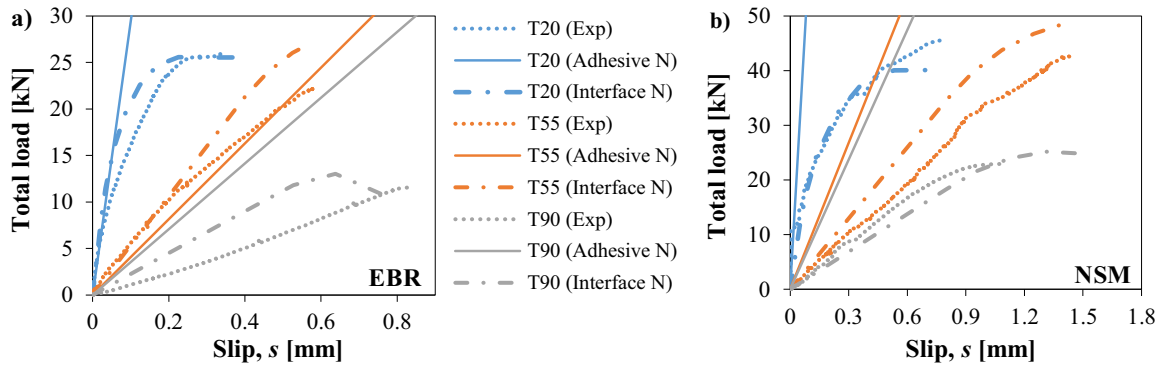

Fig. 11. Numerical (N); according to the interface and adhesive model) and experimental (Exp) total load *vs.* slip curves for the considered temperatures: a) EBR; and b) NSM specimens.

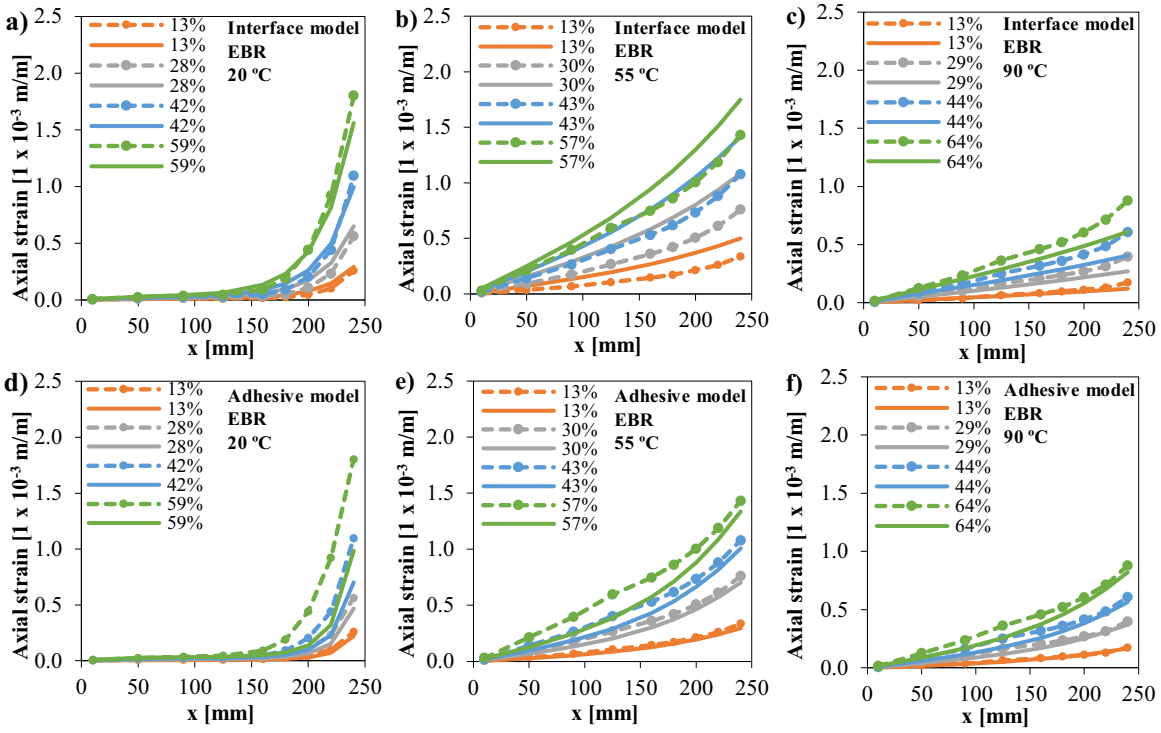

Fig. 12. Experimental (dashed) and numerical (continuous) axial strains in the EBR series for several fractions of the failure load and different temperatures: interface model (a), b) and c)) and adhesive model (d), e) and f)).

consequent smoothing of the shear stress and strain distributions along the bonded joint.

Regarding the adhesive model, although a reasonable agreement was obtained between experimental and numerical results in terms of maximum strains at the end of the CFRP strip (x = 250 mm, *cf.* Fig. 8), the linearization of the strain distributions along the bonded length with increasing temperatures is not so pronounced as in the experimental curves. In fact, as expected, the strain distributions show a more pronounced increase near the end of the bonded length, because the adhesive model exhibits a stiffer behaviour; overall, the values of the strains along the bonded length provided by the adhesive model are slightly lower than the experimental ones, with those differences being higher for the NSM technique.

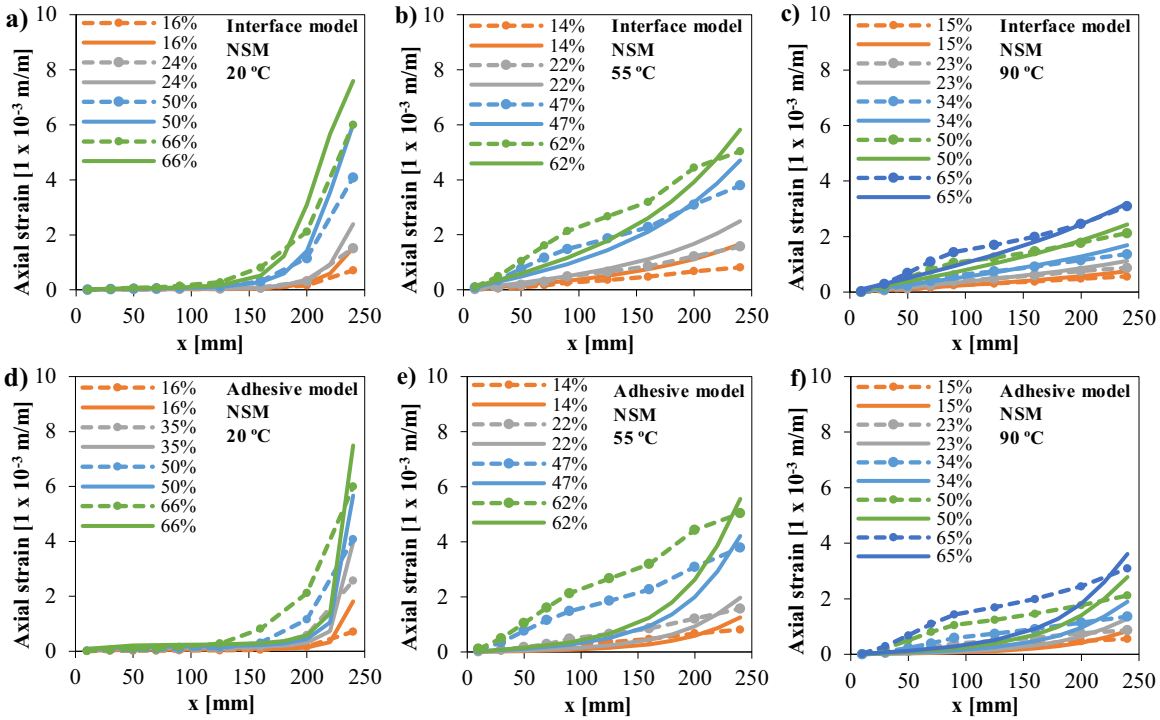

Fig. 13. Experimental (dashed) and numerical (continuous) axial strains in the EBR series for several fractions of the failure load and different temperatures: interface model (a), b) and c)) and adhesive model (d), e) and f)).

6. Conclusions

From the results obtained in the experimental study, which focused on an epoxy adhesive that is representative of most common adhesives used in CFRP strengthening systems for civil engineering applications, the following main conclusions can be drawn:

- The mechanical properties of the epoxy adhesive presents considerable reductions with increasing temperature, especially within the range that includes the glass transition process (between 42.5 and 50 °C);
- The mechanical response of the adhesive (in both tension and shear) is significantly affected by temperature – it presents linear brittle behaviour up to failure at ambient temperature, and a markedly non-linear response at higher temperatures, especially at 50 °C and 70 °C;
- The ultimate deformation capacity under tensile and shear stresses exhibits a non-monotonic variation with temperature (*i.e.*, it increases from 42.5 °C to 50 °C, and it decreases for higher temperatures), unlike the tensile and shear strengths, which decrease monotonically with temperature;
- For temperatures higher than the T_g, the stiffness degradation is significantly more pronounced than that exhibited by the corresponding strength, being almost negligible beyond 50 °C;
- The model proposed by Gibson et al., originally proposed for FRP composites, is able to accurately fit the reduction with temperature of the mechanical properties of the adhesive.

Regarding the results obtained from the numerical study, the following main conclusions can be drawn:

- The interface model was able to accurately simulate the bond behaviour, namely: (i) the non-linear load *vs.* slip response, (ii) the stress/strain peaks at the overlap end, and, with temperature increase, (iii) the linearization of the strains along the bonded length and (iv) the reduction of maximum strains.
- With the adhesive model, the assumption of a perfect connection at the interfaces provides stiffer estimates of the bond behaviour, leading to higher relative differences to test data, especially for NSM systems.
- The CFRP-concrete slip at the bonded interfaces varies significantly with temperature: at 20 °C it does not seem to be significant (*i.e.*, adhesive distortion is the governing mechanism), while with increasing temperature its relative importance progressively increases (at 90 °C it corresponds to about 70-80% of the overall slip).

Acknowledgments

The authors wish to acknowledge FCT (project PTDC/ECM-EST/1882/2014) and CERIS for funding the research and *S&P Clever Reinforcement Ibérica, Lda* for supplying the epoxy adhesive. The first author also wishes to thank the financial support of FCT through the scholarships SFRH/BDP/108319/2015. The authors thank Dr. Susana Cabral-Fonseca for her assistance with the DMA tests.

References

[1] Bakis CE, Bank LC, Brown VL, Cosenza E, Davalos JF, Lesko JJ, et al. Fibre reinforced polymer composites for construction - state-of-the-art review. J Compos Constr 2002;6(2):73–87. https://doi.org/10.1061/~ASCE!1090-0268~2002!6:2~73!.
[2] Qin G, Na J, Tan W, Mu W, Ji J. Failure prediction of adhesively bonded CFRP-Aluminum alloy joints using cohesive zone model with consideration of temperature effect. J Adhes 2018:1–24. https://doi.org/10.1080/00218464.2018.1440212.
[3] Firmo JP, Correia JR, Bisby LA. Fire behaviour of FRP-strengthened reinforced concrete structural elements: a state-of-the-art review. Compos Part B: Eng 2015;80:198–216. https://doi.org/10.1061/(ASCE)CC.1943-5614.0000535.
[4] Bascom WD, Cottington RL. Effect of temperature on the adhesive fracture behavior of an elastomer-epoxy eesin. J Adhes 1976;7(4):333–46. https://doi.org/10.1080/00218467608075063.
[5] Moussa O, Vassilopoulos AP, de Castro J, Keller T. Time–temperature dependence of thermomechanical recovery of cold-curing structural adhesives. Int J Adhes Adhes 2012;35:94–101. https://doi.org/10.1016/j.ijadhadh.2012.02.005.
[6] Blontrock H. Analysis and Modeling of the Fire Resistance of Concrete Elements with Externally Bonded FRP Reinforcement [PhD thesis in Civil Engineering]. Ghent, Belgium: Ghent University; 2003.
[7] Klamer EL, Hordijk DA, Janssen HJM. The Influence of temperature on the

debonding of externally bonded CFRP. In: Shield CK, Busel JP, Walkup SL, Gremel DD, editors. Proceedings of the 7th International Symposium on Fiber-Reinforced (FRP) Polymer Reinforcement for Concrete Structures. New Orleans, USA: American Concrete Institute; 2005. p. 1551-70.

[8] Klamer EL. Influence of Temperature on Concrete Beams Strengthened in Flexure with CFRP [Ph.D. thesis in Civil Engineering]. Eindhoven, Netherlands: Eindhoven University of Technology; 2009.

[9] Burke PJ, Bisby LA, Green MF. Effects of elevated temperature on near surface mounted and externally bonded FRP strengthening systems for concrete. Cem Concr Compos 2013;35(1):190–9. https://doi.org/10.1016/j.cemconcomp.2012.10.003.

[10] Wu ZS, Iwashita K, Yagashiro S, Ishikawa T, Hamaguchi Y. Temperature effect on bonding and debonding behavior between FRP sheets and concrete. J Soc Mater Sci 2005;54(5):474–80. https://doi.org/10.2472/jsms.54.474.

[11] Gamage JCPH, Wong MB, Al-Mahadi R. Performance of CFRP strengthened concrete members under elevated temperatures. In: Teng JF, Chen JG, editors. Proceeding of the International Sysposium on Bond Behaviour of FRP in Structures (BBFS 2005). Hong Kong, China: International Institute of FRP in Construction; 2005.

[12] Firmo JP, Pitta D, Correia JR, Tiago C, Arruda MRT. Experimental characterization of the bond between externally bonded reinforcement (EBR) CFRP strips and concrete at elevated temperatures. Cem Concr Compos 2015;60:44–54. https://doi.org/10.1016/j.cemconcomp.2015.02.008.

[13] Yu B, Kodur VKR. Effect of high temperature on bond strength of near-surface mounted FRP reinforcement. Compos Struct 2014;110:88–97. https://doi.org/10.1016/j.compstruct.2013.11.021.

[14] Firmo JP, Pitta D, Correia JR, Tiago C, Arruda MRT. Bond behavior at high temperatures between near surface mounted (NSM) CFRP strips and concrete. J Compos Constr 2015;19(4). https://doi.org/10.1061/(ASCE)CC.1943-5614.0000535.

[15] Gao W, Teng JG, Dai J. Effect of temperature variation on the full-range behavior of FRP-to-concrete bonded joints. J Compos Constr 2012;16(6):671–83. https://doi.org/10.1061/(ASCE)CC.1943-o5614.0000296.

[16] Dai J, Gao W, Teng JG. Bond-slip model for FRP laminates externally bonded to concrete at elevated temperature. J Compos Constr 2013;17(2):217–28. https://doi.org/10.1061/(ASCE)CC.1943-5614.0000337.

[17] Biscaia H, Chastre C, Viegas A, Franco N. Numerical modelling of the effects of elevated service temperatures on the debonding process of FRP-to-concrete bonded joints. Compos Part B Eng 2015;70:64–79. https://doi.org/10.1016/j.compositesb.2014.10.041.

[18] Arruda MRT, Firmo JP, Correia JR, Tiago C. Numerical modelling of the bond between concrete and CFRP laminates at elevated temperatures. Eng Struct 2016;110:233–43. https://doi.org/10.1016/j.engstruct.2015.11.036.

[19] Marques EAS, da Silva LFM, Banea MB, Carbas RJC. Adhesive joints for low- and high-temperature use: an overview. J Adhes 2015;91(7):556–85. https://doi.org/10.1080/00218464.2014.943395.

[20] ACI 440. Guide for the Design and Construction of Externally Bonded FRP Systems for Strengthening Concrete Structures, ACI 440.2R-17. Farmington Hills: American Concrete Institute; 2017.

[21] ISO 11357-1. Plastics - Diffential Scanning Calorimetry (DSC) - Part 1: General Principles. Geneve, Switzerland: International Organization for Standardization; 2009.

[22] ASTM D 5379. Standard Test Method for Shear Properties of Composite Materials by the V-Notched Beam Method. West Conshohocken, USA: American Society for Testing and Materials; 2012.

[23] Sousa JM, Correia JR, Cabral-Fonseca S. Some permanent effects of hygrothermal and outdoor ageing on a structural polyurethane adhesive used in civil engineering applications. Int J Adhes Adhes 2018;84:406–19. https://doi.org/10.1016/j.ijadhadh.2018.04.010.

[24] Sousa JM, Correia JR, Cabral-Fonseca S. Durability of an epoxy adhesive used in civil structural applications. Constr Build Mater 2018;161:618–33. https://doi.org/10.1016/j.conbuildmat.2017.11.168.

[25] Osei-Antwi M, de Castro J, Vassilopoulos AP, Keller T. Shear mechanical characterization of balsa wood as core material of composite sandwich panels. Constr Build Mater 2013;41:231–8. https://doi.org/10.1016/j.conbuildmat.2012.11.009.

[26] Garrido M, Correia JR, Keller T. Effects of elevated temperature on the shear response of PET and PUR foams used in composite sandwich panels. Constr Build Mater 2015;76:150–7. https://doi.org/10.1016/j.conbuildmat.2014.11.053.

[27] ISO 527-2. Plastics - Determination of Tensile Properties - Part 2: Test Conditions for Moulding and Extrusion Plastics. Geneve, Switzerland: International Organization for Standardization; 2012.

[28] Gibson AG, Wu YS, Evans JT, Mouritz AP. Laminate theory analysis of composites under load in fire. J Compos Mater 2006;40(7):639–58. https://doi.org/10.1177/0021998305055543.